ChemPubSoc Europe

DOI: 10.1002/chem.201600689

CHEMISTRY A European Journal Communication

Metal–Organic Frameworks

A Variety of Phase-Transition Behaviors in a Niccolite Series of $[NH_3(CH_2)_4NH_3][M(HCOO)_3]_2$

Ran Shang, Sa Chen, Ke-Li Hu, Bing-Wu Wang, Zhe-Ming Wang,* and Song Gao*[a]

Abstract: A niccolite series of $[bnH_2^{2+}][M(HCOO)_3]_2$ (bnH_2^{2+} = 1,4-butyldiammonium) shows four kinds of metal-dependent phase transitions, from high temperature para-electric phases to low-temperature ferro-, antiferro-, glass-like, and para-electric phases. The conformational flexibility of bnH_2^{2+} and the different size, mass, and bonding character of the metal ion lead to various disorder-order transitions of bnH_2^{2+} in the lattice and relevant framework modulations, thus different phase transitions and dielectric responses. The magnetic members display a coexistence or combination of electric and magnetic orderings in the low-temperature region.

Metal-organic frameworks (MOFs), now belonging to a large class of condensed matter, have shown great varieties, potentials and impacts in solid-state chemistry and physics.[1] Their inorganic–organic hybrid characters[1,2] allow the occurrence of various phase transitions, critical phenomena, and related properties, which have recently aroused great interest.[3–7] Ammonium metal formate frameworks (AMFFs) along this line are attractive.[8–18] Coexistence or synergy of magnetic and electric orderings,[9] phase transitions modulated by mixed ammoniums,[10] temperature/pressure-induced phase transitions and metal-formate bond rearrangement,[11] negative thermal expansion[9d,12] and negative compressibility,[13] and the abundant and interesting para-/ferro-/antiferro-electric (PE/FE/AFE), magnetic and mechanical properties, and so on,[9–18] have been all reported, thanks to the combination of ammonium, metal ion, and formate, which can provide the necessary elements and requirements for all of the above.[8] To date, the major explored AMFFs involve various monoammoniums, and for the series incorporating the same ammonium but different metal ions, such as $[NH_4][M(HCOO)_3]$[9a,12b,13,14] and $[(CH_3)_2NH_2][M(HCOO)_3]$,[9b,c,15] the observed phase-transition types could not be beyond two. Incorporating di-, tri-, or polyammoniums in AMFFs has been started.[8,12b,16] The conformational flexibility of polyammoniums adds another dimension, that is, the increased number of possible ordered states will probably result in more kinds of disorder-order transitions of polyammonium thus more complicated and interesting phase-transition patterns.[16c] Here we report a niccolite AMFF series of $[bnH_2^{2+}][M(HCOO)_3]_2$, in which bnH_2^{2+} is 1,4-butyldiammonium and M runs through divalent Mn, Fe, Co, Ni, Cu, Zn, and Mg. The compounds are named 1 Mn, 2 Fe, 3 Co, 4 Ni, 5 Cu, 6 Zn, and 7 Mg (3 Co and 7 Mg were reported before,[12b,16b] and the phase-transition character of 3 Co was unknown then. The data are incorporated here for comparison and completeness). The members exhibit four phase-transition patterns, from high-temperature (HT) PE to low-temperature (LT) FE (Mn and Mg), AFE (Co and Zn), glass (Fe and Ni), and PE (Cu), respectively. The relevant dielectric anomalies and relaxations strongly depend on the phase-transition character and metal. The five magnetic members display antiferromagnetic (AF) ordering in the LT region, thus combining the electric and magnetic orderings.

The seven compounds were prepared by using 1,4-butyldiamine, HCOOH, and metal perchlorate in methanol (see the Experimental Section and Table S1, in the Supporting Information).[8] Their phase purity were confirmed by powder X-ray diffraction (Figure S1, Supporting Information), and their decomposition temperatures were in the sequence of 5 Cu (385 K) < 6 Zn ~ 2 Fe (410 K) < 3 Co ~ 1 Mn ~ 4 Ni (433–437 K) < 7 Mg (470 K) (Table S2 and Figures S2a, S2b, Supporting Information). The DSC runs (Figures S2c, S2d, Supporting Information) revealed their reversible phase transitions, at the individual critical temperatures (T_C) of 345 (1 Mn), 231 (2 Fe), 246 (3 Co[16b]), 257 (4 Ni), 244 K (5 Cu; two peaks indicated probably two phase transitions), 233 (6 Zn), and 405 K (7 Mg[12b]). The DSC peaks, and the values of ΔH by integration of DSC peaks, ΔS by $\Delta S = \Delta H/T_C$ and N (the ratio of the state numbers in different phases) by $\Delta S = Rln(N)$[19] were prominent for 1 Mn, 5 Cu, and 7 Mg, less prominent for 3 Co and 6 Zn, and quite small for 2 Fe and 4 Ni. The oscillation images (OSCIs, Figure S3 to S5, Supporting Information) provided further information. On cooling, the HT single crystals of 1 Mn, 5 Cu, and 7 Mg became twinned at LT. Therefore only lattice distortions occurred. For 3 Co and 6 Zn, many weak spots appeared in LT OSCIs among the bright spots of HT OSCIs. This indicated the happening of a large, 36-fold multiple unit cell, which is still scarce.[16c] Instead, for 2 Fe

[a] R. Shang, S. Chen, K.-L. Hu, Prof. B.-W. Wang, Prof. Z.-M. Wang, Prof. S. Gao
Beijing National Laboratory for Molecular Sciences
State Key Laboratory of Rare Earth Materials Chemistry and Applications
College of Chemistry and Molecular Engineering
Peking University, Beijing 100871 (China)
E-mail: zmw@pku.edu.cn
gaosong@pku.edu.cn

Supporting information for this article can be found under http://dx.doi.org/10.1002/chem.201600689.

and 4 Ni, the HT and LT OSCIs displayed no changes. Therefore, the phase transitions of 2 Fe and 4 Ni are probably glass-like.[7a,20] All above observations implied the different, metal-dependent characters of the phase transitions within the series.

The seven compounds are all niccolite type.[12b,16a,b,17] The structures were determined at temperatures covering the phase transitions (Figure 1, and Tables S3, S4, and Figure S6 in the Supporting Information). At HT, the six members besides 5 Cu are isostructural, in trigonal space group $P\bar{3}1c$. They possess binodal 3D metal-formate frameworks containing ($4^{12}\cdot6^3$) and ($4^9\cdot6^6$) metal nodes in the ratio of 1:1, connected by *anti-anti* formates (Figure 1 a), and the framework topology is ($4^{12}\cdot6^3$)($4^9\cdot6^6$). The bnH_2^{2+} cation locates in the unique, elongated, trigonal symmetric framework cavity that is formed by two one-corner-missing cubanes twinned together (Figure 1 b and Figure S6a, Supporting Information). The cation is trigonally disordered. The terminal NH_3^+ ends and the central ethylene part are in three orientations but the two side CH_2 groups locate on the $\bar{3}$ axis, which indicates the rotating or twisting motion of bnH_2^{2+}. Each NH_3^+ site points towards to one corner cube face of the cavity, forming several N–H···O H-bonds to the formate edges. Molecular geometries are as expected, and the interatomic distances and cell parameters show the decreased trend with the metal ionic radius.[8,9a,16a,18]

The six members besides 5 Cu are classified in three groups according to their phase-transition behaviors. On cooling, 1 Mn and 7 Mg[12b] experienced a transition in which the lattice symmetry changed from the HT trigonal $P\bar{3}1c$ to LT monoclinic *Cc*. The primitive unit cell of the LT *C*-centered lattice came from the slight distortion of the HT hexagonal unit cell, by the occurred difference in *a* and *b*, and the slight derivation from 120° in γ. Below T_C, the motion of the two NH_3^+ ends of bnH_2^{2+} first froze, but the central ethylene part became swing (Figure 1 c). This alternation led to the loss of HT trigonal symmetry, and the twinning of the LT crystals. The swing motion of the central ethylene froze on further cooling, reaching the ordered state of bnH_2^{2+} in the lattice at 100 K (Figure 1 d). The cation has a zigzag middle $(CH_2)_4$ part, and the two terminal NH_3^+ ends above and below the $(CH_2)_4$ plane, showing N–C–C–C gauche conformations (assigned as *trans*-GG) with torsion angles of 68°. The transition is PE to FE, given the alternation in structural symmetry from HT nonpolar to LT polar, in Aizu notation $\bar{3}mFm$,[21] and the estimated polarizations are 1.48 (1 Mn) and 1.51 μC cm^{-2} (7 Mg) , according to the separation of the positive (NH_3^+ ends of bnH_2^{2+}) and negative (anionic framework) charges at 100 K.[12b] 3 Co and 6 Zn behaved very differently. After the transition, the lattice symmetry changed from HT $P\bar{3}1c$ to LT $R\bar{3}c$, and the LT cell 36-fold multipled the HT cell (Figure S4, Supporting Information). This is the second example of such a high-fold multiple unit cell observed to date, after $[(pnH_2^{2+})_2(H_2O)][Mg(HCOO)_3]_4$ (pnH_2^{2+} is 1,3-propane-diammonium).[16c] Such a change implied a PE to AFE transition, caused by the disorder-order alternations of bnH_2^{2+} and the related framework distortion. Below T_C, the metal-formate framework has three unique neighboring cavities A, B, and C (Figure 1 e). In 3 Co, the bnH_2^{2+} cations in A and B are ordered, and they all have the two terminal NH_3^+ ends on the same side of the plane of the zigzag middle $(CH_2)_4$ (assigned as *cis*-GG), with N–C–C–C torsion angles of 63–65°. In C, the disordered bnH_2^{2+} is in three orientations, one major (occupancy 0.72) is *cis*-GG, and the two minor (occupancy 0.14 each) nearly extended. This disorder remained down to 105 K. For 6 Zn, the situations of bnH_2^{2+} in A and C are similar, but in B the cation showed two orientations at 180 K, which then froze to one orientation at 100 K. The LT molecular and H-bonding geometries show more diversity than HT ones, due to the structural distortion. For 2 Fe and 4 Ni, the LT structures are the same as HT ones. The phase transitions are probably PE to glass-like,[20] and the bnH_2^{2+} cations randomly froze in the lattice. At LT, large Mn^{2+} and light Mg^{2+} should allow the accommodation of larger, less compact *trans*-GG bnH_2^{2+} of lower conformational energy in the frameworks, corresponding to

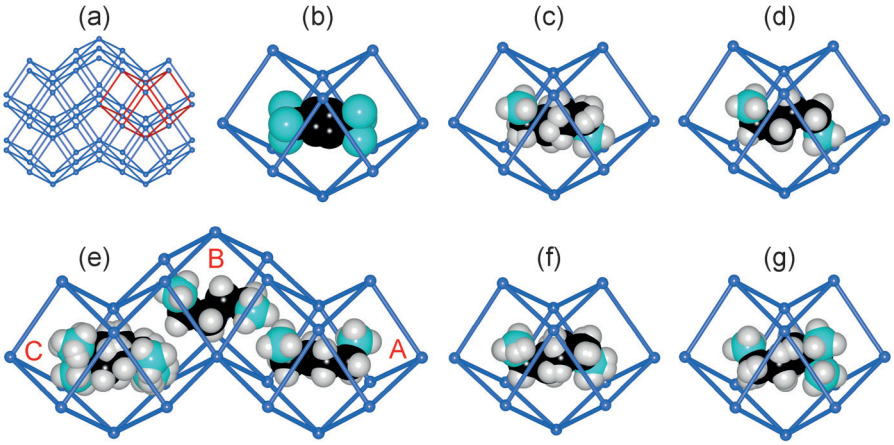

Figure 1. The structures show: a) the topological view of the niccolite metal-formate framework, with one cavity highlighted in red; b) the cavity with three-fold disordered bnH_2^{2+} inside, representing the six HT phases except 5 Cu; c) the partially disordered bnH_2^{2+} at 290 K and d) the ordered bnH_2^{2+} at 100 K in the cavity of 1 Mn (see text); e) the three neighboring cavities in 3 Co at 105 K showing the two ordered bnH_2^{2+} in cavities A and B, and one three-fold disordered bnH_2^{2+} in cavity C; the cavities in 5 Cu at 290 K f) and at 100 K g) showing different disordered states of bnH_2^{2+} (see text). Color scheme: violet blue spheres, metal nodes; violet blue bonds, formate; for bnH_2^{2+}, black, C; cyan, N; white, H; all in space-filling mode.

the PE–FE transitions with high T_C, but smaller and heaver Fe^{2+}, Co^{2+}, Ni^{2+}, and Zn^{2+} can only accommodate the smaller and compact *cis*-GG bnH_2^{2+} of higher conformational energy, thus PE–AFE/glass transitions with lower T_C. In other AMFF series, the Mn and Mg members usually have high T_C.[9,12b,13–15] The minor difference in metal size could lead to different transition characters for 2 Fe, 3 Co, 4 Ni, and 6 Zn.

5 Cu is special, as in other AMFF series.[9,14,15b,16a,18] The Jahn–Teller Cu^{2+} ions are 4+2 elongated octahedral, so the framework is composed of zigzag Cu-formate chains by short basal Cu–O_{HCOO} bonds further linked by the long axial Cu–O_{HCOO} ones (Figure S6b, 6c, Supporting Information). The HT structure is very similar to the niccolite dmenCu ($[dmenH_2^{2+}][Cu(HCOO)_3]_2$ and $dmenH_2^{2+}$ =$CH_3NH_2(CH_2)_2NH_2CH_3$),[16a] both in space group *C*2/*c*. In dmenCu, the extending $dmenH_2^{2+}$ is completely ordered in the lattice. Instead, in 5 Cu, the nearly extended bnH_2^{2+} exhibits two very closed orientations (Figure 1 f), which indicate limited swing movement of bnH_2^{2+}. After the transition, the LT phase became triclinic $P\bar{1}$, in which the unit cell came from the distorted primitive cell of the HT *C*-lattice. At LT, bnH_2^{2+} still exhibits two orientations; however, one CH_2NH_3 side was fixed, and the other side moved, with the NH_3 end flips in two positions, resulting in one *cis*-GG conformation (Figure 1 g). The transition is PE to PE, according to the above transition characters.

The four-phase transition patterns within the present series are unusual, compared to the known AMFF series[9,12b,13–15] usually showing phase-transition patterns not beyond two. The subtle synergy of the conformational flexibility of bnH_2^{2+} and the size, mass, and bonding character of the metal ion could lead to such various and interesting phase transitions.

The dielectric responses (ε' and *tan*δ) of the materials strongly depend on the transition character and metal (Figure 2, see Figure S7 and Table S2, Supporting Information). The ε' of 1 Mn quickly dropped from approximately 40 at HT to less than 10 crossing T_C, and the *tan*δ showed low values without relaxation. This is very different from 7 Mg, a relaxor that displayed strong relaxation and great enhancement of ε' for low frequencies (LF) below T_C.[12b] 1 Mn and 7 Mg experienced similar PE to FE transitions; however, the very different dielectric responses should be due to the larger and heavier Mn versus Mg, thus probably different lattice dynamics. 2 Fe, 3 Co,[16b] 4 Ni, and 6 Zn all feature strong dielectric dispersion. The HT ε' values are approximately 30 for 2 Fe, 3 Co, and 4 Ni, and 60 for 6 Zn. The ε'-descending rate on cooling changed from slow of 2 Fe to fast of 6 Zn, and stepwise behavior of decreasing developed, more significant for LF. In LT, ε' usually reached constant values of about 5. The *tan*δ versus *T* traces displayed a strong frequency (*f*) dispersion, and the *tan*δ peaks corresponded to the fall in the ε' traces due to the Kramers–Krönig relations.[22] The *tan*δ peaks went smoothly from HT–HF (high frequencies) to LT–LF for 2 Fe and 3 Co, but stepwise behaviors around T_C were clearly observed for 3 Ni and 6 Zn. The *f* versus T_P (the peak temperature in *tan*δ) data could be fitted by the Arrhenius law of $\tau = \tau_0 \times \exp(E_a/k_BT)$ ($\tau = (2\pi f)^{-1}$),[22] resulting in the activation energy E_a/k_B range of $5.5–6.3 \times 10^3$ K, or 0.47–0.54 eV, and the pre-exponential factors τ_0: $1.3–7.6 \times 10^{-16}$ s (Figure S7 h and Table S2, Supporting Information). For the four members, the rotate, twist, or flip motions of bnH_2^{2+} at HT contribute high ε' but low *tan*δ. On cooling the framework contraction and the increased H-bonding interactions slow or damp such motions then freeze into AFE or glassy states, resulting in the decrease/increase in ε'/*tan*δ and the strong dielectric dispersion. The similar E_a values are seemingly rational for the alternation of several N/C–H···O interactions required for the motions.[12b,16b,22] For 5 Cu, the swing or flip movements of bnH_2^{2+} at HT are more limited, or the amplitudes much smaller, compared to other members. Therefore, the ε' values are two or more times smaller. The decrease of ε' is quite slow, and for LF two-step descending is observed. This is because of the further limited motion of bnH_2^{2+} with one CH_2NH_3 arm fixed in the LT PE phase, but another NH_3 end still flipped. The strong *f*-dispersion of *tan*δ shows two well developed peak clusters in HT–HF and LT–LF regions, respectively, indicating different relaxation properties, corresponding to the different status of bnH_2^{2+}. However, the *f* versus T_P data could not be simulated by Arrhenius law.

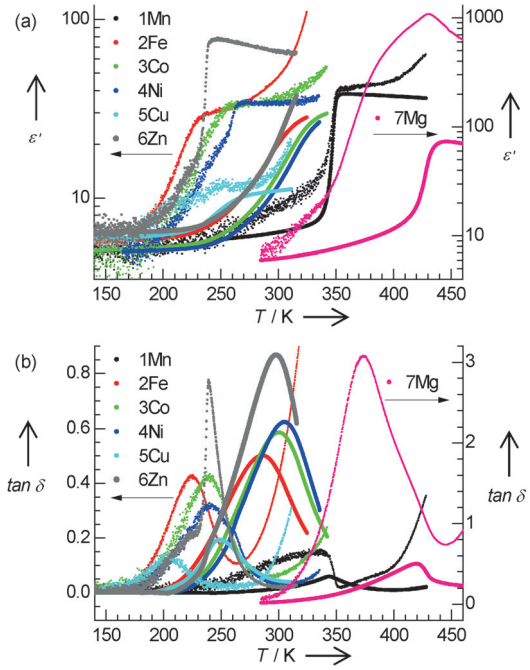

Figure 2. a) ε' versus *T* (1 k and 1 MHz) and b) *tan*δ versus *T* (5 k and 1 MHz) traces for the seven compounds, thin dot lines for 1/5 kHz and thick dot lines for 1 MHz.

The five magnetic members display typical magnetic behaviors (Figure 3, Figure S8 and Table S5, Supporting Information) of AMFFs.[8] Briefly, 1 Mn, 2 Fe, 3 Co, and 4 Ni show 3D AF ordering with weak ferromagnetism (WF) in the LT region, confirmed by the anomalies in dc susceptibilities, the zero-field-cooling and field-cooling (ZFC/FC) traces with quick rise and bifurcation behavior, the isothermal magnetizations with hysteresis, and the ac susceptibilities with peaks. The Néel temperatures are 9.1 K (1 Mn), 19.8 K (2 Fe), 9.9 K (3 Co) and 28.2 K (4 Ni), respectively, and 2 Fe possesses large coercive field and sponta-

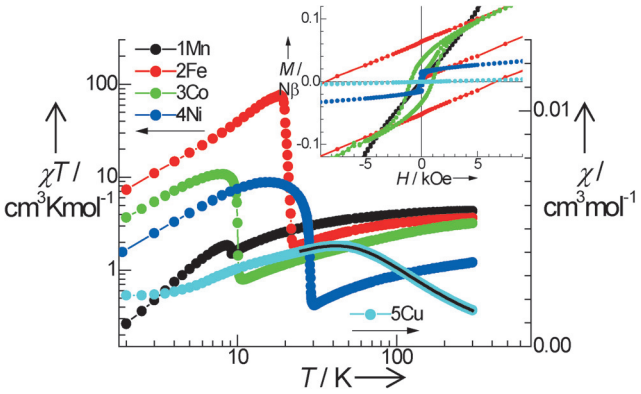

Figure 3. Plots of χT versus T under the 100 Oe field for 1 Mn to 4 Ni, and χ versus T under a 2 kOe field for 5 Cu with the black line from fitting procedure (see text); and inset, the zoomed isothermal magnetization plots at 2 K, in low field region.

neous magnetization. For 5 Cu, the Cu-formate framework consists of Cu–OCHO–Cu zigzag chains linked by the long axial Cu–$O_{formate}$ bonds. It thus exhibits low-dimensional magnetism.[11b,14,15b,16a,18] The χ versus T trace displayed a broad maximum around 43 K due to the strong intra-chain AF coupling. Then, the trace quickly further decreased down to 2 K, which indicated an inter-chain AF coupling or global AF ordering, which was further confirmed by the linear isothermal magnetization without hysteresis. Using the molecular field result,[23a] the magnetic couplings are estimated −0.43 K (1 Mn), −1.0 K (2 Fe), −4.0 K (3 Co), and −8.7 K (4 Ni). For 5 Cu, the intra- and inter-chain couplings are estimated −44.5 and −4.6 cm^{-1}, respectively, by simulating the HT susceptibilities with the Bonner–Fisher chain model.[23b]

In conclusion, a niccolite AMFF series was obtained by employing bnH_2^{2+}, in which four different phase transitions were observed. The Mn and Mg members showed PE–FE transitions with lattice symmetry changed from HT non-polar $P\bar{3}1c$ to LT polar Cc. The Co and Zn members underwent a PE–AFE phase transition from HT $P\bar{3}1c$ to LT $R\bar{3}c$ with a rare 36-fold multiple unit cell. The Fe and Ni members experienced glassy transitions without alternation in the lattice symmetry. The Cu member displayed a PE–PE transition from HT $C2/c$ to LT $P\bar{1}$. The conformational flexibility of bnH_2^{2+} combined with the different characters (size, mass, and bonding) of metal ions lead to such various disorder-order transition patterns of bnH_2^{2+} and the relevant framework modulations, thus different phase-transition characters as well as dielectric responses. The basic structural–property relationships are established. However, many details, such as the FE/AFE/glass properties, thermodynamic and critical characters of the transitions, and so on, merit further extensive investigation. In LT, the magnetic members showed coexistence or combination of various electric and magnetic states, FE/AFE/dipolar glass/PE with WF/AF. They are of further interest for MOF-multiferroics.[9] The present work demonstrates the wide variety in phase transitions and relevant properties of the AMFF class, which is becoming a good and valuable platform for relevant research.

Acknowledgement

This work was supported by the NSFC (Grants 21171010, 91422302, 21321001, 21290170 and 21290171), the National Basic Research Program of China (Grant 2013CB933401).

Keywords: diammonium metal formate · dielectricity · magnetism · metal–organic frameworks · phase transitions

[1] a) H. Furukawa, U. Müller, O. M. Yaghi, *Angew. Chem. Int. Ed.* **2015**, *54*, 3417 – 3430; *Angew. Chem.* **2015**, *127*, 3480 – 3494; b) F.-X. Coudert, *Chem. Mater.* **2015**, *27*, 1905 – 1916; c) H. Furukawa, K. E. Cordova, M. O'Keeffe, O. M. Yaghi, *Science* **2013**, *341*, 1230444 – 1 – 1230444 – 12; d) H.-C. Zhou, J. R. Long, O. M. Yaghi, *Chem. Rev.* **2012**, *112*, 673 – 674.

[2] a) A. K. Cheetham, C. N. R. Rao, *Science* **2007**, *318*, 58 – 59; b) C. N. R. Rao, A. K. Cheetham, A. Thirumurugan, *J. Phys.: Condens. Matter* **2008**, *20*, 083202.

[3] a) W. Zhang, R.-G. Xiong, *Chem. Rev.* **2012**, *112*, 1163 – 1195; b) J. S. Miller, D. Gatteschi, *Chem. Soc. Rev.* **2011**, *40*, 3065 – 3066.

[4] a) C. Lind, *Materials* **2012**, *5*, 1125 – 1154; b) Y. Wu, A. Kobayashi, G. J. Halder, V. K. Peterson, K. W. Chapman, N. Lock, P. D. Southon, C. J. Kepert, *Angew. Chem. Int. Ed.* **2008**, *47*, 8929 – 8932; *Angew. Chem.* **2008**, *120*, 9061 – 9064; c) S. G. Duyker, V. K. Peterson, G. J. Kearley, A. J. Studer, C. J. Kepert, *Nat. Chem.* **2016**, *8*, 270 – 275; d) A. B. Cairns, J. Catafesta, C. Levelut, J. Rouquette, A. van der Lee, L. Peters, A. L. Thompson, V. Dmitriev, J. Haines, A. L. Goodwin, *Nat. Mater.* **2013**, *12*, 212 – 216.

[5] T. D. Bennett, A. K. Cheetham, *Acc. Chem. Res.* **2014**, *47*, 1555 – 1562.

[6] A. U. Ortiz, A. Boutin, K. J. Gagnon, A. Clearfield, F.-X. Coudert, *J. Am. Chem. Soc.* **2014**, *136*, 11540 – 11545.

[7] a) A. B. Cairns, A. L. Goodwin, *Chem. Soc. Rev.* **2013**, *42*, 4881 – 4893; b) S. Hhorike, S. Shimomura, S. Kitagawa, *Nat. Chem.* **2009**, *1*, 695 – 704.

[8] a) R. Shang, S. Chen, Z.-M. Wang, S. Gao in *Metal-Organic Framework Materials* (Eds. L. R. Macgillivray, C. M. Lukehart), Wiley, Chichester, **2014**; b) Z.-M. Wang, K.-L. Hu, S. Gao, H. Kobayashi, *Adv. Mater.* **2010**, *22*, 1526 – 1533.

[9] a) G.-C. Xu, W. Zhang, X.-M. Ma, Y.-H. Chen, L. Zhang, H.-L. Cai, Z.-M. Wang, R.-G. Xiong, S. Gao, *J. Am. Chem. Soc.* **2011**, *133*, 14948 – 14951; b) D.-W. Fu, W. Zhang, H.-L. Cai, Y. Zhang, J.-Z. Ge, R.-G. Xiong, S. D. Huang, T. Nakamura, *Angew. Chem. Int. Ed.* **2011**, *50*, 11947 – 11951; *Angew. Chem.* **2011**, *123*, 12153 – 12157; c) P. Jain, V. Ramachandran, R. J. Clark, H. D. Zhou, B. H. Toby, N. S. Dalal, H. W. Kroto, A. K. Cheetham, *J. Am. Chem. Soc.* **2009**, *131*, 13625 – 13627; d) S. Chen, R. Shang, K.-L. Hu, Z.-M. Wang, S. Gao, *Inorg. Chem. Front.* **2014**, *1*, 83 – 98; e) L. C. Gómez-Aguirre, B. Pato-Doldán, J. Mira, S. Castro-García, M. A. Señarís-Rodríguez, M. Sánchez-Andújar, J. Singleton, V. S. Zapf, *J. Am. Chem. Soc.* **2016**, *138*, 1122 – 1125.

[10] S. Chen, R. Shang, B.-W. Wang, Z.-M. Wang, S. Gao, *Angew. Chem. Int. Ed.* **2015**, *54*, 11093 – 11096; *Angew. Chem.* **2015**, *127*, 11245 – 11248.

[11] a) E. C. Spencer, M. S. R. N. Kiran, W. Li, U. Ramamurty, N. L. Ross, A. K. Cheetham, *Angew. Chem. Int. Ed.* **2014**, *53*, 5583 – 5586; *Angew. Chem.* **2014**, *126*, 5689 – 5692; b) R. Shang, S. Chen, B.-W. Wang, Z.-M. Wang, S. Gao, *Angew. Chem. Int. Ed.* **2016**, *55*, 2097 – 2100; *Angew. Chem.* **2016**, *128*, 2137 – 2140.

[12] a) I. E. Collings, J. A. Hill, A. B. Cairns, R. I. Cooper, A. L. Thompson, J. E. Parker, C. C. Tang, A. L. Goodwin, *Dalton Trans.* **2016**, *45*, 4169 – 4178; b) R. Shang, G.-C. Xu, Z.-M. Wang, S. Gao, *Chem. Eur. J.* **2014**, *20*, 1146 – 1158.

[13] W. Li, M. R. Probert, M. Kosa, T. D. Bennett, A. Thirumurugan, R. P. Burwood, M. Parinello, J. A. K. Howard, A. K. Cheetham, *J. Am. Chem. Soc.* **2012**, *134*, 11940 – 11943.

[14] R. Shang, S. Chen, Z.-M. Wang, S. Gao, *Chem. Eur. J.* **2014**, *20*, 15872 – 15883.

[15] a) B. Pato-Doldán, M. Sánchez-Andújar, L. C. Gómez-Aguirre, S. Yáñez-Vilar, J. López-Beceiro, C. Gracia-Fernández, A. A. Haghighirad, F. Ritter, S. Castro-García, M. A. Señarís-Rodríguez, *Phys. Chem. Chem. Phys.* **2012**, *14*, 8498 – 8501; b) Z. Wang, P. Jain, K.-Y. Choi, J. van Tol, A. K. Cheetham, H. W. Kroto, H.-J. Koo, H. Zhou, J. Hwang, E. S. Choi, M.-H. Whangbo, N. S. Dalal, *Phys. Rev. B* **2013**, *87*, 224406.

[16] a) M.-Y. Li, M. Kurmoo, Z.-M. Wang, S. Gao, *Chem. Asian J.* **2011**, *6*, 3084 – 3096; b) R. Shang, S. Chen, K.-L. Hu, Z.-C. Jiang, B.-W. Wang, M. Kurmoo, Z.-M. Wang, S. Gao, *APL Materials* **2014**, *2*, 124104; c) R. Shang, Z.-M. Wang, S. Gao, *Angew. Chem. Int. Ed.* **2015**, *54*, 2534 – 2537; *Angew. Chem.* **2015**, *127*, 2564 – 2567.

[17] a) L. Cañadillas-Delgado, O. Fabelo, J. A. Rodríguez-Velamazán, M. Lemée-Cailleau, S. A. Mason, E. Pardo, F. Lloret, J. Zhao, X. Bu, V. Simonet, C. V. Colin, J. Rodríguez-Carvajal, *J. Am. Chem. Soc.* **2012**, *134*, 19772 – 19781; b) J.-P. Zhao, B.-W. Hu, F. Lloret, J. Tao, Q. Yang, X.-F. Zhang, X.-H. Bu, *Inorg. Chem.* **2010**, *49*, 10390 – 10399.

[18] K.-L. Hu, M. Kurmoo, Z.-M. Wang, S. Gao, *Chem. Eur. J.* **2009**, *15*, 12050 – 12064.

[19] M. A. White, in *Crystal Engineering: The Design and Application of Functional Solids* (Eds.: K. R. Seddon, M. Zaworotko), Kluwer Acad. Pub., Dordrecht, **1999**, p. 279.

[20] K. Binder, W. Kob, *Glassy Materials and Disordered Solids*, World Scientific Publishing, Singapore, **2005**.

[21] K. Aizu, *Phys. Rev.* **1966**, *146*, 423 – 429.

[22] A. K. Jonscher, *Dielectric Relaxation in Solids*, Chelsea Dielectrics Press, London, **1983**.

[23] a) R. L. Carlin, *Magnetochemistry*, Springer-Verlag, Heidelberg, **1986**; b) O. Kahn, *Molecular Magnetism*, VCH, Weinheim, **1993**.

Received: February 15, 2016
Published online on March 15, 2016

